Design of various controller with HES and UPFC Power Flow Controller for improved Restoration Indice

[1] R.Thirunavukkarasu [*], [2] M.Senthilkumar and [3] W.Rayez Ahamed

1Assistant Professor, Department of Electrical Engineering, Annamalai University, (On Deput GPTC-Dharmapuri), Tamil nadu, INDIA

2 Assistant Professor, Department of Mechanical Engineering, Annamalai University, (On Deput GPTC-Dharmapuri), Tamil nadu, INDIA

3Assistant Professor, Department of Electrical Engineering, Annamalai University, (On Deput GPTC-Dharmapuri), Tamil nadu, INDIA

ABSTRACT

Power system restoration problem involves status assessment, optimization of generation capability and load pickup. Quick system restoration is of prime importance not only based on the time of restoration and stability limits also play a very vital role in power system restoration problems due to unexpected load variations in power systems. Various design procedures for computing Power System Restoration Assessment Indices (PSRAI) for a Two-Area Hydro-Thermal Reheat Interconnected Power System (TAHTRIPS) in a restructured environment with a load-frequency controller optimized HES and UPF The oscillation of system frequency may sustain and grow to cause stability problems in the system if no adequate damping is provided. The disturbances to the power system due to a small load change can even result in wide deviation in system frequency which is referred as load-frequency control problem. The simple conventional PI^2 controllers are still popular in power industry for frequency regulation as in case of any change in system operating conditions new gain values can be computed easily even for multi-area power systems. Quick system restoration is of prime importance not only based on the time of restoration and also stability limits also plays a very vital role in power system restoration problems due to unexpected load variations in power systems. This paper computation of various PSRAI for TAH (with mechanical governor) -TRIPS and TAH (with Electric governor)- TRIPS unit based on the settling time concept, The design of the PI^2 controller gains are tuned using HES and UPF implemented to achieve a fast restoration time in the output responses of the system when the system experiences with various step load perturbations. In this paper the PRSAI are calculated for different types of possible transactions and the necessary remedial measures to be adopted and improving the system .

Keywords: *PI^2 ,HES ,UPFC, Electric Governor, Power System Restoration Assessment Indices, Load- Frequency Control, Restructured Power System.*

INTRODUCTION

The electric power can be bought and sold between the interconnected VIU through the tie-lines and moreover such interconnection should provide greater reliability [1]. The major change that had happened is with the emergence of Independent Power Producer (IPP) that can sell power to VIU. In the restructure environment it is generally agreed that the first step is to separate the generation of power from the transmission and distribution companies, thus putting all the generation on the same footing as the IPP [2]. In an interconnected power system, a sudden load perturbation in any area causes the deviation of frequencies of all the areas and also in the tie-line powers. This has to be corrected to ensure the generation and distribution of electric power companies to ensure good quality. This can be achieved by optimally tuning Load-Frequency controller gains. Many investigations in the area of Load-Frequency Control (LFC) problem for the interconnected power systems have been reported over the past six decades. A number of control strategies have been employed in the design of load-frequency controllers in order to achieve better dynamic performance. The efficient incorporation of controllers will modify the transient response and steady state error of the system. Among the various types of load-frequency controllers, the most widely employed is the conventional Proportional plus Integral controller (PI^2). A lot of studies have been made related to LFC in a deregulated environment over last decades. These studies try to modify the conventional LFC system to take into account the effect of bilateral contracts on the dynamics [3] and improve the dynamical transient response of the system [4-7] under various operating conditions. With the restructured electric utilities, the Load-Frequency Control requirements especially the nominal frequency in an interconnected power system besides maintaining the net interchange of power between control areas at predetermined values should be enhanced to ensure the quality of the power system. The importance of decentralized controllers for multi area load-frequency control in the restructured environment, where in, each area controller uses only the local states for feedback, is well known. The stabilization of frequency oscillations in an interconnected power system becomes challenging whenimplemented in the future competitive environment. So advanced economic, high efficiency and improved control schemes [8, 9] are required to ensure the power system reliability for which PSRAI can be used In this paper various methodologies were adopted in computing Power System Restoration Assessment Indices (PSRAI) for Two-Area Hydro (with Mechanical/Electrical governor) Thermal Reheat Interconnected Power System (TAHTRIPS) in a restructured environment. With the various Power System Restoration Assessment Indices (Feasible Restoration Indices, Comprehensive Restoration Indices) the remedial measures to be taken can be adjudged like integration of additional spinning reserve, incorporation of effective intelligent controllers, load shedding etc.The restoration process of the bulk-power transmission system following a partial or a total blackout has two main issues during a restoration; these are voltage control and frequency control [10]. Special attention is therefore given to the behavior of network parameters, control equipments as they affect the voltage and frequency regulation during the restoration process which in turn reflects in PSRAI. During restoration due to wide fluctuations in the frequency and voltage it becomes very difficult to maintain the integrity in the system. Inability to control the frequency may lead to unsuccessful restoration. The repeated collapse of the system Islands due to tripping of generators due to either over frequency or under frequency condition causes delay in getting normalcy [10] Now-a-days the complexities in the power system are being solved with the use of Evolutionary Computation (EC) such as Differential Evolution (DE) [11], Genetic Algorithms (GA),

Practical Swarm Optimizations (PSO) [12] and Ant Colony Optimization (ACO) [13], which are some of the heuristic techniques having immense capability of determining global optimum. Classical approach based optimization for controller gains is a trial and error method and extremely time consuming when several parameters have to be optimized simultaneously and provides suboptimal result. Some authors have applied GA to optimize the controller gains more efficiently, but the premature convergence of GA degrades its search capability [14]. Recent research has brought out some deficiencies in using GA, PSO based techniques [14, 15]. The Bacterial Foraging Optimization [BFO] mimics how bacteria forage over a landscape of nutrients to perform parallel non gradient optimization [16]. The BFO algorithm is a computational intelligence based technique that is not affected larger by the size and nonlinearity of the problem and can be convergence to the optimal solution in many problems where most analytical methods fail to converge. This more recent and powerful evolutionary computational technique BFO [16] is found to be user friendly and is adopted for simultaneous optimization of several parameters for both primary and secondary control loops of the governor.

To obtain the best convergence performance, an effective cost function is derived using the tie-line power and frequency deviations of the control areas and their rates of changes according to time integral. The main function of LFC is to regulate a signal called Area Control Error (ACE), which accounts for error in the frequency as well as the errors in the interchange power with neighboring areas. Conventional Load-Frequency Control uses a feedback signal that is either based on the Integral of ACE or is based on ACE and it's Integral. In this study, BFO algorithm is used to optimizing the Proportional plus Integral (PI^2) controller gains for the load frequency control of a Two-Area Hydro-Thermal Reheat Interconnected Power System (TAHTRIPS) in a restructured environment. Various case studies are analyzed to develop Power System Restoration Assessment Indices (PSRAI) namely, Feasible Restoration Index (FRI) and Complete Restoration Index (CRI) which are able to predict the normal operating mode, emergency mode and restorative modes of the power system.

2. TWO-AREA HYDRO-THERMAL REHEAT INTERCONNECTED POWER SYSTEM (TAHTRIPS) IN RESTRUCTURED

Load-Frequency Control (LFC) plays a very important role in power system and its main role is to maintain load-generation balance. Many investigations in the field of LFC for an interconnected system have been reported in literature over past few decades, which emphasizes on LFC pertaining to a thermal system and relatively a lesser attention has been contributed towards the LFC of a Hydro-Thermal system of widely different characteristics [17-22]. In this paper, investigation has been carried out for a TAHTIPS in which small perturbations was made to occur in area-1 and in area-2 and their impact on optimum selection of controller gain settling

In the restructured competitive environment of power system, the Vertically Integrated Utility (VIU) no longer exists. The deregulated as been assessed based on the various Restoration Indices. power system consists of GENCOs, DISCOs, and Transmissions Companies (TRANSCOs) and Independent System Operator (ISO). GENCOs which will compete in a free market to sell the electricity they produce..With the emergence of the distinct identities of GENCOs, TRANSCOs, DISCOs and the ISO, many of the ancillary services of a VIU will

have a different role to play and hence have to be modeled differently. Among these ancillary service controls one of the most important services to be enhanced is the Load-frequency control [23]. The LFC in a deregulated electricity market should be designed to consider different types of possible transactions, such as poolco-based transactions, bilateral transactions and a combination of these two [24]. In the new scenario, a DISCO can contract individually with a GENCO for acquiring the power and these transactions will be made under the supervision of ISO. To make the visualization of contracts easier, the concept of "DISCO Participation Matrix" (DPM) is used which essentially provides the information about the participation of a DISCO in contract with a GENCO. In DPM, the number of rows has to be equal to the number of GENCOs and the number of columns has to be equal to the number of DISCOs in the system. Any entry of this matrix is a fraction of total load power contracted by a DISCO toward a GENCO. As a results total of entries of column belong to DISCOi of DPM is $\sum_i cpf_{ij} = 1$. In this study two- area interconnected power system in which each area has two GENCOs and two DISCOs. Let GENCO 1, GENCO 2, DISCO 1, DISCO 2 be in area 1 and GENCO 3, GENCO 4, DISCO 3, DISCO 4 be in area 2 as shown in Fig 1.The corresponding DPM is given as follows

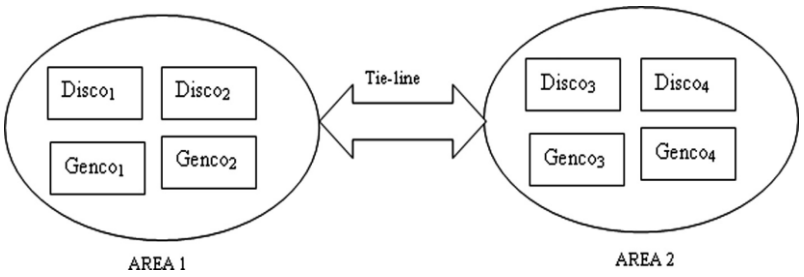

Fig .1 Schematic diagram of two-area system in restructured environment

$$DPM = \begin{bmatrix} & DISCO & & \\ cpf_{11} & cpf_{12} & cpf_{13} & cpf_{14} \\ cpf_{21} & cpf_{22} & cpf_{23} & cpf_{24} \\ cpf_{31} & cpf_{32} & cpf_{33} & cpf_{34} \\ cpf_{41} & cpf_{42} & cpf_{43} & cpf_{44} \end{bmatrix} \begin{matrix} \\ G \\ E \\ N \\ C \\ O \end{matrix} \quad (1)$$

Where *cpf* represents "Contract Participation Factor" and is like signals that carry information as to which the GENCO has to follow the load demanded by the DISCO. The linearized model of a two-area Hydro- Thermal reheat interconnected power system in deregulated environment is shown in Fig.2. The actual and scheduled steady state power flow through the tie-line is given as

$$\Delta P_{tie1-2,\,scheduled} = \sum_{i=1}^{2}\sum_{j=3}^{4} cpf_{ij}\Delta P_{L\,j} - \sum_{i=3}^{4}\sum_{j=1}^{2} cpf_{ij}\Delta P_{L\,j} \quad (2)$$

And at any given time, the tie-line power error

$\Delta P_{tie1-2,\,error}$ is defined as (3)

$$\Delta P_{tie1-2,\,error} = \Delta P_{tie1-2,\,actual} - \Delta P_{tie1-2,\,scheduled} \quad (4)$$

The error signal is used to generate the respective ACE signals as in the traditional scenario

$$ACE_1 = \beta_1 \Delta F_1 + \Delta P_{tie\,1-2,\,error} \quad (5)$$

$$ACE_2 = \beta_2 \Delta F_2 + \Delta P_{tie\,2-1,\,error} \quad (6)$$

For two area system as shown in Fig.1, the contracted power supplied by i[th] GENCO is given as

$$\Delta Pg_i = \sum_{j=1}^{DISCO=4} cpf_{ij} \Delta PL_j \quad (7)$$

Also note that $\Delta PL_{1,LOC} = \Delta PL_1 + \Delta PL_2$ and $\Delta PL_{2,LOC} = \Delta PL_3 + \Delta PL_4$. In the proposed LFC implementation, contracted load is fed forward through the DPM matrix to GENCO set points. The actual loads affect system dynamics via the input $\Delta PL_{,LOC}$ to the power system blocks. Any mismatch between actual and contracted demands will result in frequency deviations that will drive LFC to re dispatch the GENCOs according to ACE participation factors, i.e., apf_{11}, apf_{12}, apf_{21} and apf_{22}. The state space representation of the minimum realization model of 'N' area interconnected power system may be expressed as [25].

$$\begin{aligned} \dot{x} &= Ax + Bu + \Gamma d \\ y &= Cx \end{aligned} \quad (8)$$

Where $x = [x_1^T, \Delta p_{ei} \ldots x_{(N-1)}^T, \Delta p_{e(N-1)} \ldots x_N^T]^T$, n - state vector

$$n = \sum_{i=1}^{N} n_i + (N-1)$$

$u = [u_1, \ldots u_N]^T = [\Delta P_{C1} \ldots P_{CN}]^T$, N - Control input vector

$d = [d_1, \ldots d_N]^T = [\Delta P_{D1} \ldots P_{DN}]^T$, N - Disturbance input vector , $2N$ - Measurable output vector

where A is system matrix, B is the input distribution matrix, Γ is the disturbance distribution matrix, C is the control output distribution matrix, x is the state vector, u is the control vector and d is the disturbance vector consisting of load changes.

As stated earlier, in the Hydro power plan, the electric governor operation is very fast in nature than that of the system used with mechanical governors as the speed sensing, droop compensation and computing functions are performed electrically. The output signal drives electro-mechanical transducer, which operates a pilot valve and pilot valve servo motor. The turbine rotor speed is measured electronically with high accuracy [23]. And, here in this case study it is used as a feedback controller which drives the plant to be controlled within a weighted sum of error and integral of that value.

3.1 Design of Proportional-Integral Controller

The conventional Proportional-Integral (PI) controller, Proportional control reduces the peak over-shoot in the damping oscillations of system response and Integral control provides zero state error in frequency deviation

and tie line power flow. In load frequency control nominal parameters of system is achieved with the generation of proper control signal by the PI controller is given by

$$u(t) = K_P \ ACE(t) + \frac{K_P}{T_i} \int ACE(t)\, dt \tag{8}$$

Proportional controller is used to reach the steady state condition much quicker because of the fast transient response with proportional controller. The proportional term of the controller produces a control signal proportional to the Area control Error (ACE) in the system, so that $u(t) = K_P \ ACE(t)$ where K_P is the proportional gain. Typically, given a step change of load demand, low values of K_P give rise to stable responses with large steady-state errors. Higher values of K_P give better steady-state performance, but worse transient response. Therefore, the higher value of K_P is used to reduce the steady state error, although increasing the gain K_P decreases the system time constant and damping. But, if the gain of integrator K_I is sufficiently high, overshoot will occur increasing sharply as a function of the gain, this is highly undesirable. Lower value of K_I reduces overshoot but increases rise time of the system. Based upon discussion it is required to design both the K_P and K_I properly.

3.2. Design of Proportional-Double Integral (PI^2) controller

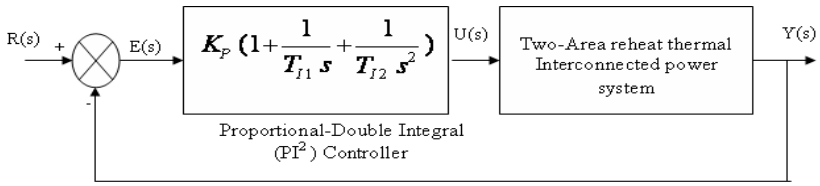

Fig.2 closed loop control structure for AGC loop using PI^2 controller

The ability of proportional integral (PI) controllers to compensate most practical industrial processes has led to their wide acceptance in industrial applications. The ideal continuous time domain PI controller for a single input single output process is expressed in the Laplace domain as follows:

$$G_c(s) = k_P \ (1 + \frac{1}{T_i \ s}) \tag{9}$$

with T_i = integral time constant. If $T_i = \infty$ (i.e. P control), then the closed loop measured value will always be less than the desired value for processes without an integrator term, as a positive error is necessary to keep the measured value constant, and less than the desired value. However, there are a number of disadvantages to the ultimate cycle tuning approach:(i) the system must generally be destabilized under proportional control, (ii) the empirical nature of the method means that uniform performance is not achieved in general, (iii) several trials must typically be made to determine the ultimate gain, (iv) the resulting process upsets may be detrimental to product quality (v) there is a danger of misinterpreting a limit cycle as representing the stability limit and the amplitude of the process variable signal may be so great that the experiment may not be carried out for cost or safety considerations. So no long term error, as the two gains are tuned.The disadvantage of adopting integral controller alone is that it tends to make the system unstable because it responds slowly towards the produced error. A controller with two integrators is required to reduce this error to zero. Belanger and Luyben [10] had undertaken an analytical approach for tuning the Proportional-Double Integral (PI^2) controllers and relate the

prescribed tuning parameters to the ultimate gain and period of the plant [10]. Simple formulae were used to define the tuning parameters for PI^2 controller and the settings are given by $K_P = 0.33K_u$, $T_{I1} = 2.26\,T_u$, $T_{I2} = 20.5\,T_u^2$ [11]. This study is based on a numerical optimization approach rather than an algebraic one, and uses a more general error metric than damping ratio. The effect of the restriction relating the two controller integral time constants can be examined since optimal tunings with and without the restriction can be calculated. Additionally, faster systems can be controlled using this approach since true first order responses are allowed by the chosen model form, in contrast to the more limited type of responses available when the model is restricted to consist of only one integrator. In this study Proportional-Double Integral (PI^2) controllers is used for AGC loop of an interconnected power system as shown in Fig.2. The PI^2 controllers are expressed in Laplace form as follows [10]:

$$G_c(s) = k_P\ (1 + \frac{1}{T_{I1}\ s} + \frac{1}{T_{I2}\ s^2}) \tag{10}$$

In this work optimum gain values are tuned based on Area Control Error of the output response of the system (especially the frequency deviation and tie-line power deviation) and with these gain values the performance of the system is analyzed. And here in this case study it is used as a feedback controller which drives the plant to be controlled within a weighted sum of error and integral of that value i.e. it produces an output signal consisting of three terms one proportional to error signal and the other proportional to integral of error signal. In order to satisfy the above requirements, PI^2 controller gains in the LFC loop are to be optimized using BFO algorithm. In the present work Integral Square Error (ISE) criterion [24] is used to minimize the objective function [J]. The objective function is minimized using Bacterial Foraging Optimization Technique and are represented

$$U_1 = -K_p\ ACE_1 - K_{I1}\int ACE_1\ dt - K_{I2}\int ACE_1\ dt$$

$$U_2 = -K_p\ ACE_{21} - K_{I1}\int ACE_2\ dt - K_{I2}\int ACE_2\ dt \tag{11}$$

The relative simplicity of this controller is a successful approach towards the zero steady state error in the frequency of the system.

Application of HES and UPFC units for AGC in Deregulated Environment Design of various controllers

4.1 Hydrogen Energy Storage System (HESS)

Generally the optimization of the schedule of distributed energy sources depends on the constraints of the problem which are load limits, actual generation capabilities, status of the battery, forecasted production schedule. Hydrogen is a serious contender for future energy storage due to its versatility. Consequently, producing hydrogen from renewable resources using electrolysis is currently the most desirable objective available.

4.1.1 Aqua Electrolyzer for production of Hydrogen

An aqua electrolyzer is a device that produces hydrogen and oxygen from water. Water electrolysis is a reverse process of electrochemical reaction that takes place in a fuel cell. An aqua electrolyzer converts dc electrical energy into chemical energy stored in hydrogen. From electrical circuit point of view, an aqua electrolyzer can be considered as a voltage-sensitive nonlinear dc load. For a given aqua electrolyzer, within its rating range, the higher the dc voltage applied, the larger is the load current. That is, by applying a higher dc voltage, more H_2

can be generated. In this paper, the aqua electrolyzer is considered as a subsystem which absorbs the rapidly fluctuating output power. It generates hydrogen and stores in the hydrogen tank and this hydrogen is used as fuel for the fuel cell.

4.1.2 Constant electrolyzer power

The effects of operating the electrolyzer at constant power has to be studied which is the common practice for conventional electrolysis plants. The electrolyzer and the hydrogen storage tanks are designed so that no wind energy is dissipated, and the amount of hydrogen obtained is more efficient. The electrolyzer rating is decided to be equal to [18]

$$P_e^{\max} = p_w^{\max} - P_g^{\max} - \min\left(P_i\ (t)\right) \tag{12}$$

The hydrogen storage tanks are sized according to the following criterion [18].

$$0 < V_H(t) - V_H^{\max} \qquad for \quad t = 1....N \tag{13}$$

so that the hydrogen storage does not reach the lower and upper limits during the simulation period. For each of the hydrogen-load scenarios, simulations have been run for different wind power capacities. The required hydrogen storage capacity for the different hydrogen-filling scenarios and wind power capacities have to be obtained which results in a nonlinear relationship between the required hydrogen storage and the installed wind power. It can be noted that for a fixed wind power capacity, a lower hydrogen-filling rate leads to larger hydrogen storage as with the normal operating conditions.The transfer function can be expressed as first order lag:

$$G_{AE}\ (s)\ =\ \frac{K_{AE}}{1+sT_{AE}} \tag{14}$$

The energy produced by the various types of cells depends on the operation temperature, the type of fuel cell, and the catalyst used. Fuel cells do not produce any pollutants and have no moving parts. The transfer function of Fuel Cell (FC) can be given by a simple linear equation as

$$G_{FC}\ (s)\ =\ \frac{K_{FC}}{1+sT_{FC}} \tag{15}$$

Hydrogen is one of the promising alternatives that can be used as an energy carrier. The universality of hydrogen implies that it can replace other fuels for stationary generating units for power generation in various industries. Having all the advantages of fossil fuels, hydrogen is free of harmful emissions when used with dosed amount of oxygen, thus reducing the greenhouse effect [19]. Essential elements of a hydrogen energy storage system The over all transfer function of hydrogen Energy storage unit has can be

$$G_{HES}\ (s)\ =\ \frac{K_{HES}}{1+sT_{HES}} = \frac{K_{AE}}{1+sT_{AE}} * \frac{K_{FC}}{1+sT_{FC}} \tag{16}$$

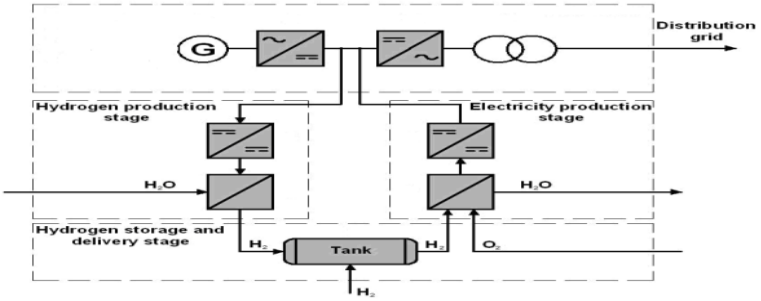

Fig 4 Block diagram of the hydrogen storage unit

4.2 Mathematical Model of UPFC unit

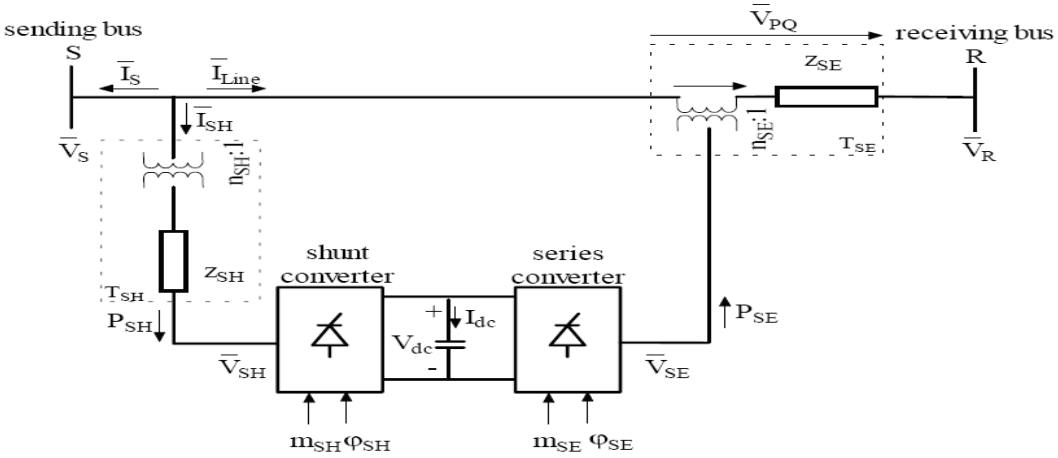

Fig.5 Fundamental frequency model of UPFC

The UPFC is a device placed between two busses referred to as the UPFC sending bus and the UPFC receiving bus. It consists of two Voltage-Sourced Converters (VSCs) with a common DC link. For the fundamental frequency model, the VSCs are replaced by two controlled voltage sources as shown in Fig.5 [23]. The voltage source at the sending bus is connected in shunt and will therefore be called the shunt voltage source. The second source, the series voltage source, is placed between the sending and the receiving busses. The UPFC is placed on high-voltage transmission lines. This arrangement requires step-down transformers in order to allow the use of power electronics devices for the UPFC. Applying the Pulse Width Modulation (PWM) technique to the two VSCs the following equations for magnitudes of shunt and series injected voltages are obtained

$$V_{SH} = m_{SH} \frac{V_{DC}}{2\sqrt{2} n_{SH} V_B} \tag{17}$$

$$V_{SE} = m_{SE} \frac{V_{DC}}{2\sqrt{2} n_{SE} V_B} \tag{18}$$

Where: m_{SH} – Amplitude modulation index of the shunt VSC control signal, m_{SE} – Amplitude modulation index of the series VSC control signal, n_{SH} – shunt transformer turn ratio, n_{SE} – Series transformer turn ratio,

V_B – The system side base voltage in kV, V_{DC} – DC link voltage in kV. The phase angles of V_{SH} and V_{SE} are

$$\delta_{SH} = \angle(\delta_S - \varphi_{SH})$$
$$\delta_{SE} = \angle(\delta_S - \varphi_{SE}) \quad (19)$$

Where φ_{SH} is the firing angle of the shunt VSC with respect to the phase angle of the sending bus voltage, φ_{SE} is the firing angle of the series VSC with respect to the phase angle of the sending end bus Voltage. The series converter injects an AC voltage $V_{SH} = V_{SE}\angle(\delta_S - \varphi_{SE})$ in series with the transmission line. Series voltage magnitude V_{SE} and its phase angle φ_{SE} with respect to the sending bus which is controllable in the range of $0 \leq V_{SE} \leq V_{SE\max}$ and $0 \leq \varphi_{SE} \leq 360^0$.

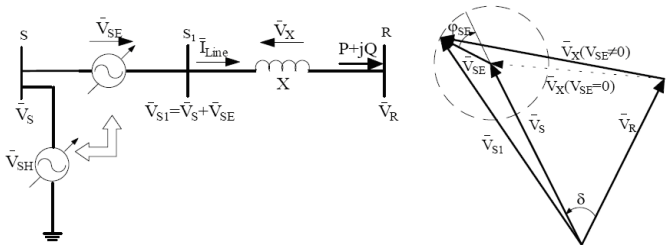

Fig 6. Application of UPFC in the tie-line

The shunt converter injects controllable shunt voltage such that the real component of the current in the shunt branch balance the real power demanded by the series converter. The real power can flow freely in either direction between the AC terminals. On the other hand as the reactive power cannot flow through the DC link, it is being absorbed or generated locally by each converter. The shunt converter operated to exchange the reactive power with the AC system provides the possibility of independent shunt compensation for the line. If the shunt injected voltage is regulated to produce a shunt reactive current component that will keep the sending end bus voltage at its pre-specified value, then the shunt converter is operated in the Automatic Voltage Control Mode. Shunt converter can also be operated in the Var Control Mode. In this case shunt reactive current is produced to meet the desired inductive or capacitive Var requirement. UPFC is placed in the transmission line connecting buses S and R as shown in Fig 6 [23]. Line conductance was neglected. UPFC is represented by two ideal voltage sources of controllable magnitude and phase angle. Bus S and fictitious bus S_1 are shown in Fig 6 which represents UPFC' s sending and receiving buses respectively. In this case, the complex power received at the receiving end of the line is given by

$$S = \overline{V_R}\ \bar{I}_{Line}^{*} = \bar{V}_R\left(\frac{\bar{V}_S + \bar{V}_{SE} - \bar{V}_R}{jX}\right)^{*} \quad (20)$$

Where $\overline{V_{SE}} = V_{SE}\angle(\delta_S - \varphi_{SE})$

The complex conjugate of this complex power is

$$S^{*} = P - jQ = \overline{V_R}^{*}\left(\frac{\overline{V_S} + \overline{V}_{SE} - \overline{V_R}}{jX}\right) \quad (21)$$

Performing simple mathematical manipulations and separating real and imaginary components of (21) the following expressions for real and the reactive powers received at the receiving end of the line are

$$P = \frac{V_S V_R}{X}\sin\delta + \frac{V_R V_{SE}}{X}\sin(\delta - \varphi_{SE}) = P_O(\delta) + P_{SE}(\delta, \varphi_{SE})$$

$$Q = -\frac{V_R^{\ 2}}{X} + \frac{V_S V_R}{X}\cos\delta + \frac{V_R V_{SE}}{X}\cos(\delta - \varphi_{SE}) = Q_O(\delta) + Q_{SE}(\delta, \varphi_{SE}) \quad (22)$$

For V_{SE} = 0 the above equations represent the real and reactive powers of the uncompensated system. As the UPFC series voltage magnitude can be controlled between 0 and V_{SE} max, and its phase angle can be controlled between 0 and 360 degrees at any power angle, and using in (22) the real and reactive power received at bus R for the system with the UPFC unit is installed can be controlled between rotation of the series injected voltage phasor with RMS value of V_{SEmax} from 0 to 360^0 allows the real and the reactive power flow to be controlled within the boundary

$$P_{\min}(\delta) \le P \le P_{\max}(\delta)$$

$$Q_{\min}(\delta) \le Q \le Q_{\max}(\delta) \quad (23)$$

System modelling for control design

The HES and UPFC units are found to be superior to the governor system in terms of the response speed against, the frequency fluctuations. Therefore, the operational tasks are assigned according to the response speed as follow. the governor system acts for compensating the steady state error of the frequency deviations. Fig 7 shows the model for the control design of HES and UPFC units. governor is much slower than that of HES or UPFC units. Then the state equation of the system represented by Fig 7 becomes

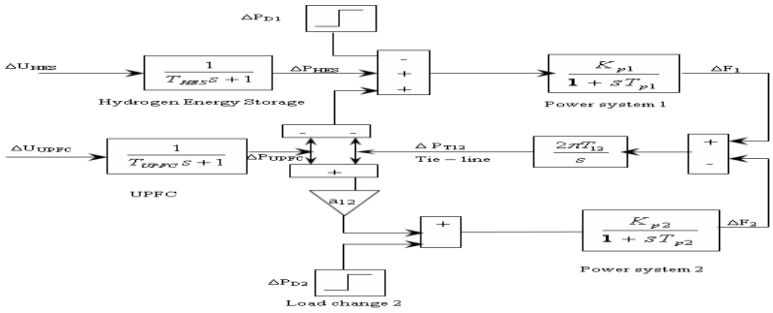

Fig. 7 Linearized reduction model for the control design

$$\begin{bmatrix} \Delta\dot{F}_1 \\ \Delta\dot{P}_{T12} \\ \Delta\dot{F}_2 \end{bmatrix} = \begin{bmatrix} -\frac{1}{T_{p1}} & -\frac{k_{p1}}{T_{p1}} & 0 \\ 2\pi T_{12} & 0 & -2\pi T_{12} \\ 0 & \frac{a_{12}\,k_{p2}}{T_{p2}} & -\frac{1}{T_{p2}} \end{bmatrix} \begin{bmatrix} \Delta F_1 \\ \Delta P_{T12} \\ \Delta F_2 \end{bmatrix} + \begin{bmatrix} \frac{k_{p1}}{T_{p1}} & -\frac{k_{p1}}{T_{p1}} \\ 0 & 0 \\ 0 & \frac{a_{12}\,k_{p2}}{T_{p2}} \end{bmatrix} \begin{bmatrix} \Delta P_{HES} \\ \Delta P_{UPFC} \end{bmatrix} \quad (24)$$

Here, from the physical view point it is noted that the UPFC located between two areas is effective to stabilize the inter-area oscillation mode only, and then the HES which is capable of supplying the energy into the power system can be utilized for the control of the inertia mode.

5.1 Control design of Hydrogen Energy Storage unit

The design process starts from the reduction of two area system into one area which represents the Inertia centre mode of the overall system. The controller of HES is designed in the equivalent one area system to reduce the frequency deviation of inertia centre. The equivalent system is derived by assuming the synchronizing coefficient T_{12} to be large. From the state equation of $\Delta\dot{P}_{T12}$ in (24)

$$\frac{\Delta\dot{P}_{T12}}{2\pi T_{12}} = \Delta F_1 - \Delta F_2 \tag{25}$$

Setting the value of T_{12} in (25) to be infinity yields $\Delta F_1 = \Delta F_2$. Next, by multiplying state equation of $\Delta\dot{F}_1$ and $\Delta\dot{F}_2$ in (24) by $\frac{T_{p1}}{k_{p1}}$ and $\frac{T_{p2}}{a_{12}\, k_{p2}}$ respectively, then

$$\frac{T_{p1}}{k_{p1}}\Delta\dot{F}_1 = -\frac{1}{k_{p1}}\Delta F_1 - \Delta P_{T12} - \Delta P_{UPFC} + \Delta P_{HES} \tag{26}$$

$$\frac{T_{p2}}{a_{12}\, k_{p2}}\Delta\dot{F}_2 = \frac{-1}{k_{p_2}\, a_{12}}\Delta F_2 + \Delta P_{T12} + \Delta P_{UPFC} \tag{27}$$

By summing (26) and (27) and using the above relation $\Delta F_1 = \Delta F_2 = \Delta F$

$$\Delta\dot{F} = \frac{\left(-\frac{1}{k_{p1}} - \frac{1}{k_{p2}a_{12}}\right)}{\left(\frac{T_{p1}}{k_{p1}} + \frac{T_{p2}}{k_{p2}a_{12}}\right)}\Delta F + \frac{1}{\left(\frac{T_{p1}}{k_{p1}} + \frac{T_{p2}}{k_{p2}a_{12}}\right)}\Delta P_{HES} + C\Delta P_D \tag{28}$$

Where the load change in this system ΔP_D is additionally considered, here the control $\Delta P_{RFB} = -K_{HES}\,\Delta F$ is applied then.

$$\Delta F = \frac{C}{s + A + K_{HES}\, B}\Delta P_D \tag{29}$$

Where $A = \left(-\frac{1}{k_{p1}} - \frac{1}{k_{p2}a_{12}}\right) \Big/ \left(\frac{T_{p1}}{k_{p1}} + \frac{T_{p2}}{k_{p2}a_{12}}\right); B = \frac{1}{\left[\frac{T_{p1}}{K_{p1}} + \frac{T_{p2}}{K_{p2}a_{12}}\right]}$

Where C = proportionality constant between change in frequency and change in load demand. Since the control purpose of HES is to suppress the deviation of ΔF quickly against the sudden change of ΔP_D In (29) the final values with K_{HES} = 0 and with $K_{HES} \neq 0$ are C/A and C/(A+K_{HES} B) respectively therefore the percentage reduction is represented by

$$C/(A + K_{HES}\, B)/(C/A) = R/100 \tag{30}$$

For a given R, the control gain of HES unit is calculated as

$$K_{HES} = \frac{A}{BR}(100 - R) \tag{31}$$

5.2 Control design of Unified Power Flow Controller unit

The controller for the UPFC is design to enhance the damping of the inter-area mode. In order to extract the inter-area mode from the system in (24), the concept of overlapping decompositions is applied. First, the state

variables of the system (24) are classified into three groups, i.e. $x_1 = [\Delta F_1]$, $x_2 = [\Delta P_{T12}]$, $x_3 = [\Delta F_2]$. next, the system (24) is decomposed into two decoupled subsystems. Where the state variable ΔP_{T12} is duplicated included in both subsystems, which is the reason that this process is called overlapping decompositions. Then, one subsystem which preserves the inter-area mode is represented by.

$$\begin{bmatrix} \Delta\dot{F}_1 \\ \Delta\dot{P}_{T12} \end{bmatrix} = \begin{bmatrix} -\frac{1}{T_{p1}} & \frac{-Kp_1}{T_{p1}} \\ 2\pi T_{12} & 0 \end{bmatrix} \begin{bmatrix} \Delta F_1 \\ \Delta P_{T12} \end{bmatrix} + \begin{bmatrix} \frac{-Kp_1}{T_{p1}} \\ 0 \end{bmatrix} [\Delta P_{UPFC}] \tag{32}$$

The control purpose of the UPFC is to damp the peak value of frequency deviation in area 1 after a sudden change in the load demand. Since the system (32) is the second order oscillation system, the percentage overshoot *Mp (new)* can be specified for the control design. *Mp (new)* is given as a function of the damping ratio by

$$M_{p(new)} = e^{(-\pi\delta/\sqrt{1-\delta^2})} \tag{33}$$

The real and imaginary parts of eigenvalue after the control are expressed by

$$\alpha_s = \delta\omega_n \tag{34}$$

$$\beta_s = \omega_n\sqrt{1-\delta^2} \tag{35}$$

Where w_n is the undamped natural frequency, by specifying *Mp* and assuming $\beta_s = \beta$, the desired pair of eigenvalue is fixed. As a result, the eigenvalue assignment method derives to feed back scheme as

$$\Delta P_{UPFC} = -k_1 \Delta F_1 - k_2 \Delta P_{T12} \tag{36}$$

The characteristic polynomial of the system (32) with state feedback, which is given by

$$|\lambda I - (A - BK)| = 0 \tag{37}$$

Where state feedback gain matrix $K = [k_1, k_2]$. The desired characteristic polynomial from the specified eigenvalue (μ_1, μ_2) is given by

$$(\lambda - \mu_1)(\lambda - \mu_2) = 0 \tag{38}$$

By equating the coefficients of (37) and (38) the elements k_1, k_2 of state feedback gain matrix K are obtained.

5.3 Structure of UPFC-based damping controller

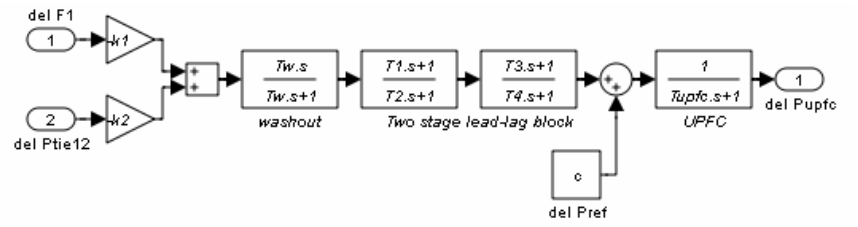

Fig.8 Structure of UPFC-based damping controller

The active power controller of UPFC has a structure of Lead-Lag compensator with output signal ΔP_{ref}. In this study the dynamic characteristics of UPFC is modeled as the first order controller with time constant T_{upfc} . It is to be noted that the injected power deviations of UPFC, ΔP_{upfc} acting positively for area 1 and reacts negatively for area 2. Therefore ΔP_{upfc} flow into both of the areas with different signs (+,-) simultaneously. The commonly used Lead-Lag structure is chosen in this study as UPFC based supplementary damping controller as shown in Fig 8.

Power System Restoration

Power system disturbances are most likely to occur as the result of loss of generating units, transmission facilities, or as the result of unexpected load changes. However, the steps taken to do so be achieved with the coordinated control action with the System Operator so as to solve the problem in a best manner. In this study two-area interconnected reheat thermal in a restructured environment without and with HES and UPFC units are considered. More over Power System Restoration Indices namely Feasible Restoration Indices (FRI) when the system is operating in a normal condition with Gencos units in operation and Comprehensive Restoration Indices (CRI) are one or more Gencos unit outage in any area. The Feasible Restoration Indices 1 (ε_1) is obtained as the ratio between the settling time of frequency deviation in area 1 (ς_{s1}) and power system time constant (T_{p1}) of area 1

$$\varepsilon_1 = \frac{\varsigma_{s1}}{T_{p1}} \tag{39}$$

The Feasible Restoration Indices 2 (ε_2) is obtained as the ratio between the settling time of frequency deviation in area 2 (ς_{s2}) and power system time constant (T_{p2}) of area 2

$$\varepsilon_2 = \frac{\varsigma_{s2}}{T_{p2}} \tag{40}$$

The Feasible Restoration Indices 3 (ε_3) is obtained as the ratio between the settling time of Tie –line power deviation (ς_{s3}) and synchronous power coefficient T_{12}

$$\varepsilon_3 = \frac{\varsigma_{s3}}{T_{12}} \tag{41}$$

The Feasible Restoration Indices 4 (ε_4) is obtained as the peak value frequency deviation $\Delta F_1(\varsigma_p)$ response of area 1 exceeds the final value $\Delta F1(\varsigma_s)$

$$\varepsilon_4 = \Delta F_1(\varsigma_p) - \Delta F_1(\varsigma_s) \tag{42}$$

The Feasible Restoration Indices 5 (ε_5) is obtained as the peak value frequency deviation $\Delta F_2(\varsigma_p)$ response of area 2 exceeds the final value $\Delta F2(\varsigma_s)$

$$\varepsilon_5 = \Delta F_2(\varsigma_p) - \Delta F_2(\varsigma_s) \tag{43}$$

The Feasible Restoration Indices 6 (ε_6) is obtained as the peak value tie-line power deviation $\Delta P_{tie}(\varsigma_p)$ response exceeds the final value $\Delta P_{tie}(\varsigma_s)$

$$\varepsilon_6 = \Delta P_{tie}(\varsigma_p) - \Delta P_{tie}(\varsigma_s) \tag{44}$$

The Feasible Restoration Indices 7 (ε_7) is obtained from the peak value of the control input deviation $\Delta P_{c1}(\varsigma_p)$ response of area 1 with respect to the final value $\Delta P_{c1}(\varsigma_s)$

$$\varepsilon_7 = \Delta P_{c1}(\varsigma_p) - \Delta P_{c1}(\varsigma_s) \tag{45}$$

The Feasible Restoration Indices 8 (ε_8) is obtained from the peak value of the control input deviation $\Delta P_{c2}(\varsigma_p)$ response of area 2 with respect to the final value $\Delta P_{c2}(\varsigma_s)$

$$\varepsilon_8 = \Delta P_{c2}(\varsigma_p) - \Delta P_{c2}(\varsigma_s) \tag{46}$$

The optimal controller gains and their performance of the system various case studies the corresponding the Comprehensive Restoration Indices (CRI) ($\varepsilon_9, \varepsilon_{10}, \varepsilon_{11}, \varepsilon_{12}, \varepsilon_{13}, \varepsilon_{14}, \varepsilon_{15}, \varepsilon_{16}$) is obtained from (39- 46).

Simulation Results and Observations

In this test system all the Gencos in each area consists of thermal reheat units with different capacity and the active power model of HES is places in area 1 and UPFC unit located in series with the tie-line is shown in Fig.9. The nominal parameters are given in Appendix [27]. The control parameters of HES and TCPS are shown in the Table 1. Then PI controller gain values (K_{Pi} $K_{I\,i,}$) and PI^2 controller gain values (K_{Pi}, $K_{I1i,}$ $K_{I\,2i}$) for each area and parameters of UPFC unit ($T_{UPFC,}$ T_1, T_2, T_3 and T_4) are optimized are tuned simultaneously with help of BFO algorithm for both traditional and bilateral based LFC schemes in TATRIPS with a wide range of load changes for different case studies. The results are obtained by MATLAB 7.01 software and 50 iterations are chosen for the convergence of the solution in the BFO algorithm.

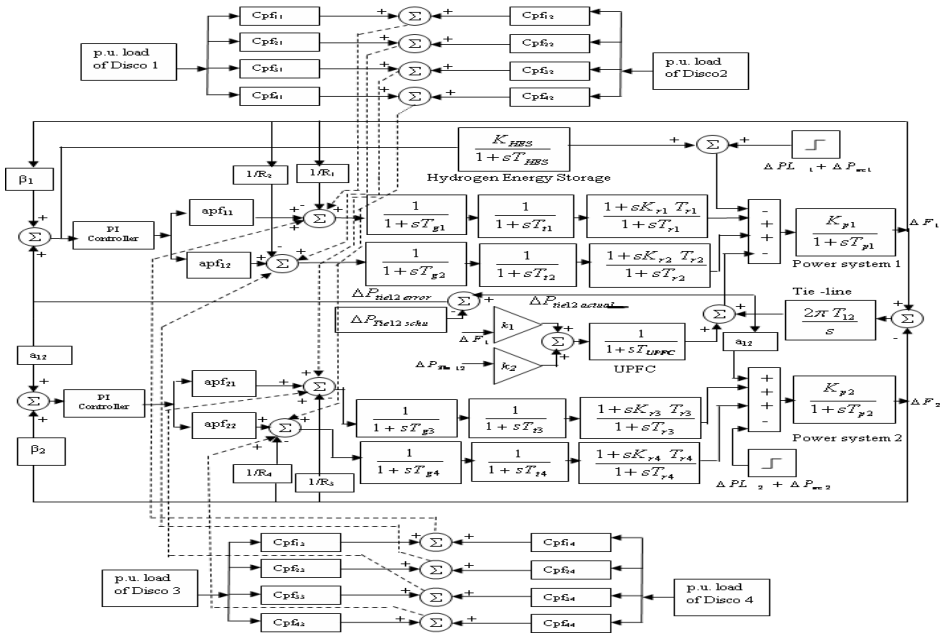

Fig. 9 Linearized model of a two-area Thermal reheat interconnected power system in a restructured environment with HES and UPFC unit

7.1 Feasible Restoration Indices

7.7.1: Poolco based transaction

In this scenario, Gencos participate only in the load following control of their areas. It is assumed that a large step load 0.1 pu MW is demanded by each Disco in area 1. Assume that a case of Poolco based contracts between Dicos and available Gencos is simulated based on the following Disco Participation Matrix (DPM) referring to Eq (1) is considered as

$$DPM = \begin{bmatrix} 0.5 & 0.5 & 0 & 0 \\ 0.5 & 0.5 & 0 & 0 \\ 0 & 0 & 0 & 0 \\ 0 & 0 & 0 & 0 \end{bmatrix} \quad (47)$$

$Disco_1$ and $Disco_2$ demand identically from their local Gencos, viz., $Genco_1$ and $Genco_2$. Therefore, $cpf_{11} = cpf_{12} = 0.5$ and $cpf_{21} = cpf_{22} = 0.5$. It may happen that a Disco violates a contract by demanding more power than that specified in the contract and this excess power is not contracted to any of the Gencos. This uncontracted power must be supplied by the Gencos in the same area to the Disco. It is represented as a local load of the area but not as the contract demand. Consider scenario-1 again with a modification that Disco demands as given in Table 2 and 3. From the simulation results Power System Restoration Indices namely Feasible Restoration Indices are evaluated using in (39)-(46) from dynamic output responses of the proposed test system TATRIPS without HES/ UPFC using either PI or PI^2 controller is shown in Table 4 and 5 respectively and test system TATRIPS with HES and UPFC using PI^2 controller is shown in Table 6 (case 1- 4).

7.1.2: Bilateral transaction

Here all the Discos have contract with the Gencos and the following Disco Participation Matrix (DPM) be considered.

$$DPM = \begin{bmatrix} 0.5 & 0.25 & 0.5 & 0.4 \\ 0.2 & 0.25 & 0.2 & 0.2 \\ 0.0 & 0.3 & 0.2 & 0.25 \\ 0.3 & 0.2 & 0.1 & 0.15 \end{bmatrix} \quad (48)$$

In this case, the $Disco_1$, $Disco_2$, $Disco_3$ and $Disco_4$, demands 0.15 pu.MW, 0.05 pu.MW, 0.15 pu.MW and 0.05 pu.MW from Gencos as defined by cpf in the DPM matrix and each Gencos participates in LFC as defined by the following ACE participation factor $apf_{11} = apf_{12} = 0.5$ and $apf_{21} = apf_{22} = 0.5$. The comparative transient performances of two-area Power System with HES and UPFC using PI^2 controller for given load perturbation as shown in Fig 10 and it can observed that the oscillations in the area frequencies and tie-line power deviation have decreased to a considerable extent as compare to that of the system without HES and UPFC units. The corresponding Feasible Restoration Indices are calculated from dynamic output responses of the proposed test system TATRIPS without HES and UPFC using either PI or PI^2 controller is shown in Table 4 and 5 respectively and test system TATRIPS with HES and UPFC using PI^2 controller is shown in Table 6 (case 5- 8).

V. CONCLUSION

Design procedure for obtaining Power System Restoration Assessment Indices (PSRI) which indicates the requirements to be adopted in minimizing the frequency deviations, tie-line power deviation of a two-area interconnected restructured power system to ensure the reliable operation of the power system. In these PSRI can be utilized to help system operators in real time by suggesting relevant actions taken to adhere for the

automation of the power system restoration. Traditional PI and the proposed PI^2 controllers are designed using BFO algorithm and implemented in a restructured power system. The proposed PI^2 controllers, represents a version of the classical PI controller, where an extra feedback signal and Integral term is added. The effectiveness of the proposed PI^2 controller is tested in a two-area deregulated power system for a wide range of load demands and disturbances under different operating conditions. The proposed PI^2 controller shows better performance to ensure improved PSRI in order to provide reduce the restoration time, thereby improving the system reliability than PI controller. BFO Algorithm is found to be easy to implement without additional computational complexity, with quite promising results and ability to jump out the local optima. Moreover the dynamic output responses of first peak frequency deviation of both areas and tie-line power oscillations following sudden load disturbances in either of the areas can be suppressed a controlling the phase angle of UPFC unit. Then HES unit contributes a lot in promoting the efficiency of the overall generation control through load leveling and the assurance of LFC capacity after overload characteristic and quick responsiveness. From the simulated results it is also observed that the restoration process for the Thermal generating unit with HES and UPFC units are more sophisticated control for a better restoration of the power system output responses .

II.ACKNOWLEDGEMENT

The authors wish to thank the authorities of Annamalai University, Annamalainagar, Tamilnadu, India for the facilities provided to prepare this paper.

Table 1 Results obtained based on the control design with HES and UPFC units

1	Gain value of HES unit (31) K_{HES} = 0.902
2	Eigenvalue of system without UPFC (32) λ1 = - 0.25 +j 1.8081 λ2 = - 0.25 – j 1.8081
3	Inter-area mode, without UPFC Mp = 64.85%
4	Design specification, with UPFC Mp(new) =5 %
5	New Eigenvalue of the system with UPFC (32) λ1(new) = -1.724 + j1.8081 λ2(new) = -1.724 - j1.8081
6	State Feed back Gain value of UPFC (36) $[K_1,K_2]$= [-0.566, -0.908]

Table 2 Optimized Controller parameters of the TATRIPS using PI controller for the corresponding Load demand change

TATRIPS	PI controller gain of Area 1		PI controller gain of Area 2		Load demand in pu.MW				un contracted load demand pu.MW	
	K_P	K_I	K_P	K_I	$Disco_1$	$Disco_2$	$Disco_3$	$Disco_4$	Area1	Area 2
Case 1	0.341	0.459	0.191	0.081	0.1	0.1	0.0	0.0	0.0	0.0
Case 2	0.384	0.315	0.121	0.051	0.1	0.1	0.0	0.0	0.1	0.0

Case 3	0.411	0.489	0.284	0.112	0.1	0.1	0.0	0.0	0.0	0.1
Case 4	0.386	0.352	0.256	0.127	0.1	0.1	0.0	0.0	0.1	0.1
Case 5	0.316	0.512	0.127	0.296	0.15	0.05	0.15	0.05	0.0	0.0
Case 6	0.393	0.575	0.131	0.305	0.15	0.05	0.15	0.05	0.1	0.0
Case 7	0.324	0.492	0.214	0.362	0.15	0.05	0.15	0.05	0.0	0.1
Case 8	0.381	0.563	0.249	0.368	0.15	0.05	0.15	0.05	0.1	0.1
Case 9	0.421	0.685	0.247	0.183	0.12	0.08	0.14	0.06	0.0	0.0
Case 10	0.438	0.696	0.255	0.178	0.12	0.08	0.14	0.06	0.1	0.0
Case 11	0.416	0.671	0.252	0.172	0.12	0.08	0.14	0.06	0.0	0.1
Case 12	0.435	0.678	0.261	0.186	0.12	0.08	0.14	0.06	0.1	0.1

Table 3 Optimized Controller parameters of the TATRIPS using PI^2 controller for the corresponding Load demand change

TATRIPS	PI^2 controller gain of Area 1			PI^2 controller gain of Area 2			Load demand in pu.MW				un contracted load demand pu.MW	
	K_P	K_{I1}	K_{I2}	K_P	K_{I1}	K_{I2}	$Disco_1$	$Disco_2$	$Disco_3$	$Disco_4$	Area 1	Area 2
Case 1	0.113	0.067	1.12×10^{-2}	0.063	0.012	5.51×10^{-4}	0.1	0.1	0.0	0.0	0.0	0.0
Case 2	0.127	0.046	4.16×10^{-3}	0.039	0.007	3.47×10^{-4}	0.1	0.1	0.0	0.0	0.1	0.0
Case 3	0.136	0.071	9.35×10^{-3}	0.094	0.016	7.12×10^{-4}	0.1	0.1	0.0	0.0	0.0	0.1
Case 4	0.127	0.052	5.17×10^{-3}	0.085	0.018	1.02×10^{-3}	0.1	0.1	0.0	0.0	0.1	0.1
Case 5	0.104	0.075	1.33×10^{-2}	0.041	0.043	1.11×10^{-2}	0.15	0.05	0.15	0.05	0.0	0.0
Case 6	0.129	0.085	1.35×10^{-2}	0.043	0.044	1.14×10^{-2}	0.15	0.05	0.15	0.05	0.1	0.0
Case 7	0.107	0.072	1.21×10^{-2}	0.071	0.053	9.86×10^{-3}	0.15	0.05	0.15	0.05	0.0	0.1
Case 8	0.126	0.082	1.34×10^{-2}	0.082	0.054	8.76×10^{-3}	0.15	0.05	0.15	0.05	0.1	0.1
Case 9	0.139	0.101	1.79×10^{-2}	0.082	0.027	2.18×10^{-3}	0.12	0.08	0.14	0.06	0.0	0.0
Case 10	0.144	0.102	1.78×10^{-2}	0.084	0.026	2.01×10^{-3}	0.12	0.08	0.14	0.06	0.1	0.0
Case 11	0.137	0.098	1.75×10^{-2}	0.083	0.025	1.89×10^{-3}	0.12	0.08	0.14	0.06	0.0	0.1
Case 12	0.143	0.086	1.71×10^{-2}	0.086	0.027	2.13×10^{-3}	0.12	0.08	0.14	0.06	0.1	0.1

Table 4 FRI for TATRIPS using PI controller for different types of case studies

TATRIPS	FRI based on Settling time (ς_s)			FRI based on Peak over/ under shoot (m_p)			FRI based on control input deviation (ΔP_c)	
	ε_1	ε_2	ε_3	ε_4	ε_5	ε_6	ε_7	ε_8
Case 1	0.871	0.861	42.63	0.351	0.316	0.042	0.149	0.113
Case 2	0.936	0.875	43.54	0.562	0.402	0.053	0.234	0.124
Case 3	0.901	0.943	46.23	0.432	0.459	0.062	0.143	0.252
Case 4	1.212	1.375	53.63	0.624	0.716	0.081	0.225	0.236
Case 5	0.923	0.896	40.78	0.357	0.456	0.072	0.153	0.093
Case 6	0.949	0.912	41.96	0.553	0.513	0.076	0.264	0.146
Case 7	0.931	0.986	45.51	0.381	0.653	0.081	0.159	0.162
Case 8	1.245	1.312	52.29	0.633	0.991	0.085	0.258	0.178

Table 5 FRI for TATRIPS using PI^2 controller for different types of case studies

TATRIPS	FRI based on Settling time (ς_s)			FRI based on Peak over/ under shoot (m_p)			FRI based on control input deviation (ΔP_c)	
	ε_1	ε_2	ε_3	ε_4	ε_5	ε_6	ε_7	ε_8
Case 1	0.853	0.837	40.12	0.336	0.294	0.033	0.126	0.096
Case 2	0.915	0.851	41.88	0.541	0.382	0.046	0.213	0.106
Case 3	0.881	0.927	44.91	0.413	0.438	0.051	0.126	0.231
Case 4	1.192	1.332	51.42	0.596	0.702	0.073	0.208	0.219

Case 5	0.901	0.871	38.24	0.309	0.396	0.058	0.113	0.053
Case 6	0.923	0.892	39.73	0.524	0.453	0.061	0.223	0.105
Case 7	0.914	0.961	42.22	0.367	0.618	0.067	0.124	0.119
Case 8	1.224	1.294	50.74	0.608	0.949	0.069	0.213	0.136

Table 6 FRI for TATRIPS with HES and UPFC unit using PI^2 controller for different types of case studie

TATRIPS	FRI based on Settling time (ς_s)			FRI based on Peak over/ under shoot (m_p)			FRI based on control input deviation (ΔP_c)	
	ε_1	ε_2	ε_3	ε_4	ε_5	ε_6	ε_7	ε_8
Case 1	0.568	0.653	20.57	0.183	0.217	0.012	0.046	0.068
Case 2	0.635	0.665	23.28	0.391	0.311	0.016	0.153	0.085
Case 3	0.591	0.689	24.63	0.317	0.369	0.021	0.076	0.198
Case 4	0.723	0.989	31.58	0.441	0.638	0.043	0.152	0.185
Case 5	0.579	0.697	19.36	0.098	0.212	0.028	0.045	0.031
Case 6	0.621	0.766	22.25	0.308	0.352	0.041	0.166	0.081
Case 7	0.662	0.831	24.97	0.168	0.474	0.043	0.073	0.009
Case 8	0.851	0.993	30.09	0.402	0.725	0.048	0.152	0.102

Table 7 CRI for TATRIPS using PI controller with different types of case studies

TATRIRPS	CRI based on Settling time (ς_s)			CRI based on Peak over / under shoot (M_p)			CRI based on control input deviation (ΔP_c)	
	ε_9	ε_{10}	ε_{11}	ε_{12}	ε_{13}	ε_{14}	ε_{15}	ε_{16}
Case 9	1.431	1.537	55.48	0.678	0.719	0.156	0.185	0.161
Case 10	1.715	1.678	56.39	0.691	0.701	0.167	0.193	0.167
Case 11	1.525	1.823	59.36	0.705	0.929	0.168	0.187	0.173
Case 12	1.747	1.867	59.29	1.317	1.252	0.173	0.218	0.186

Table 8 CRI for TATRIPS using PI^2 controller with different types of case studies

TATRIRPS	CRI based on Settling time (ς_s)			CRI based on Peak over / under shoot (M_p)			CRI based on control input deviation (ΔP_c)	
	ε_9	ε_{10}	ε_{11}	ε_{12}	ε_{13}	ε_{14}	ε_{15}	ε_{16}
Case 9	1.386	1.456	54.96	0.503	0.514	0.131	0.182	0.159
Case 10	1.702	1.598	55.13	0.559	0.611	0.148	0.191	0.165
Case 11	1.511	1.736	58.54	0.573	0.836	0.151	0.183	0.169
Case 12	1.716	1.771	58.87	1.185	1.122	0.167	0.215	0.184

Table 9 CRI for TATRIPS with HES and UPFC unit using PI^2 controller with different types of case studies

TATRIRPS	CRI based on Settling time (ς_s)			CRI based on Peak over / under shoot (M_p)			CRI based on control input deviation (ΔP_c)	
	ε_9	ε_{10}	ε_{11}	ε_{12}	ε_{13}	ε_{14}	ε_{15}	ε_{16}
Case 9	0.891	1.224	44.75	0.224	0.238	0.091	0.091	0.119

Case 10	1.114	1.275	45.14	0.238	0.351	0.101	0.101	0.128
Case 11	0.998	1.488	47.36	0.375	0.468	0.112	0.105	0.142
Case 12	1.197	1.597	49.85	1.001	1.003	0.129	0.116	0.151

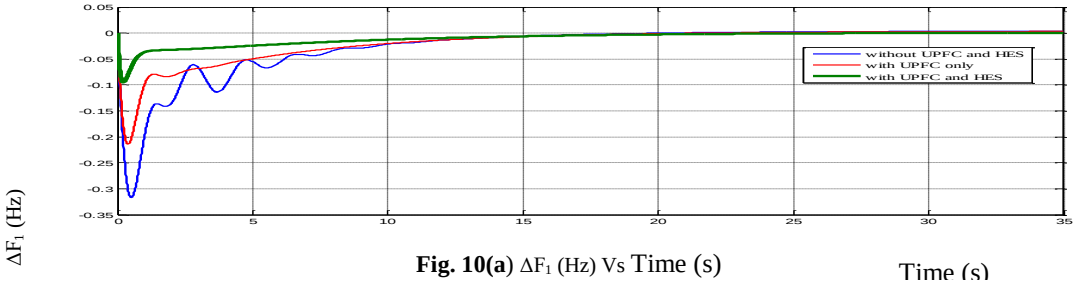

Fig. 10(a) ΔF_1 (Hz) Vs Time (s)

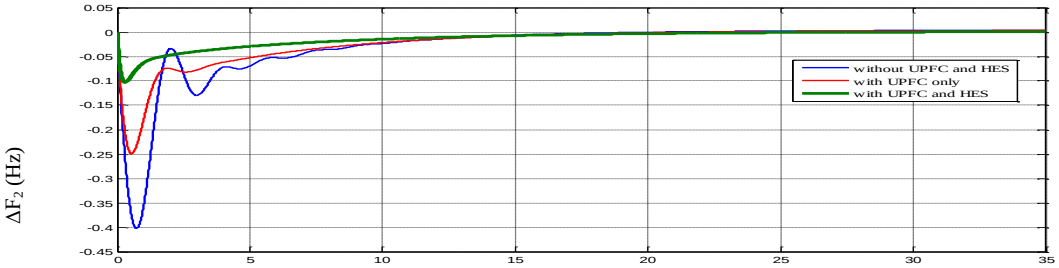

Fig.10 (b) ΔF_2 (Hz) Vs Time (s)

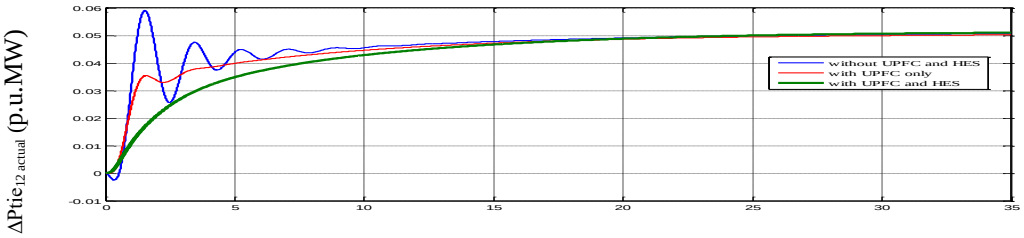

Fig.10 (c) $\Delta Ptie_{12,\ actual}$ (p.u.MW) Vs Time (s)

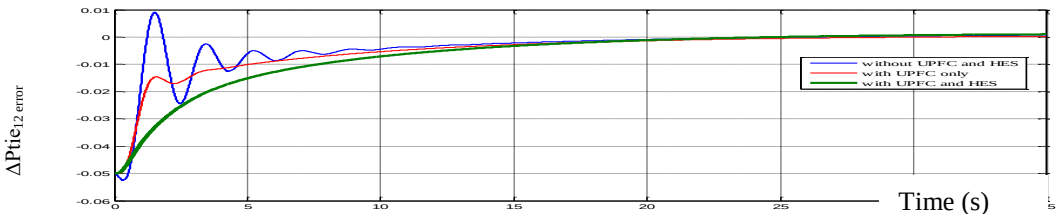

Fig.10(d) $\Delta Ptie_{12,\ error}$ (p.u.MW) Vs Time (s)

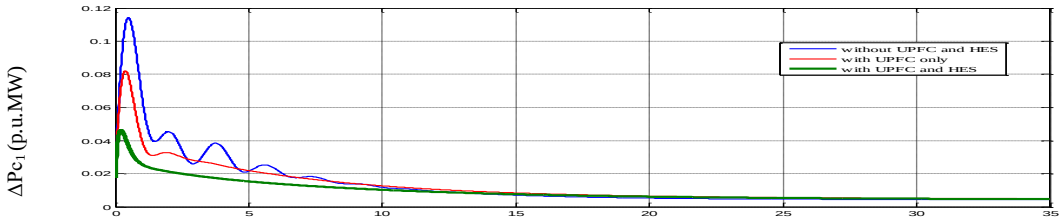

Fig.10 (e) ΔPc_1 (p.u.MW) Vs Time (s)

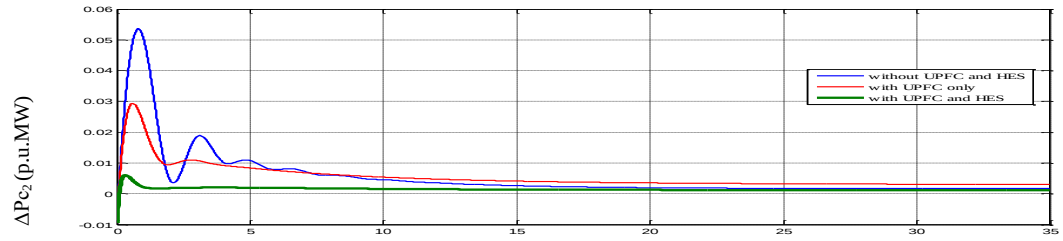

Fig.10 (f) ΔPc_2 (p.u.MW) Vs Time (s)

Time (s)

Fig.10 Dynamic responses of the frequency deviations, tie- line power deviations, and Control input deviations for a two area LFC system without and with HES and UPFC unit using PI^2 controllers in the restructured scenario-2 bilateral based transactions.

REFERENCES

[1] Mukta, Balwinder Singh Surjan, Load Frequency Control of Interconnected Power System in Deregulated Environment: A Literature Review, International Journal of Engineering and Advanced Technology 2(3) (2013) 435-441

[2] B.Delfino, F.Fornari, S.Massucco, Load-frequency control and inadvertent interchange evaluation in restructured power systems, IEE Proceedings-Generation Transmission and Distribution 149(5) (2002) 607-614.

[3] A.P.Fathima, M.A.Khan, Design of a new market structure and robust controller for the frequency regulation services in the deregulated power system, Electrical Power Components and Systems 36(8) (2008) 864-883.

[4] H. Bevrani, Y. Mitani, K. Tsuji, Robust decentralized LFC in a restructured power system, Energy Conversion and Management, 45 (2004) 2297-2312.

[5] V. Donde, M. A. Pai, I. A. Hiskens, Simulation and optimization in an AGC system after deregulation, IEEE Transactions on Power Systems 16 (3) (2001) 481-489.

[6] L. S. Rao, N.V. Ramana, Recent Philosophies of AGC of a Hydro-thermal System in Deregulated Environment, International Journal of Advances in Engineering and Technology 2(1) (2012) 282-288.

[7] Shaik Farook, P. Sangmeswara Raju, Decentralized Fractional Order PID Controller for AGC in a Multi Area Deregulated Power System, International Journal of Advances in Electrical and Electronics Engineering 1(3) (2013) 317-333.

[8] Lalit Chandra Saikia, J. Nanda, S. Mishra, Performance comparison of several classical controllers in AGC for multi-area interconnected thermal system, Electrical Power and Energy Systems 33 (2011) 394-401.

[9] J.Nanda A.Mangla, S.Suri, Some new findings on automatic generation control of an interconnected hydrothermal system with conventional controllers, IEEE Transactions on Energy Conversion 21 (2006) 187-194.

[10] P. Belanger, W. Luyben, Design of low-frequency compensator for improvement of plant wide regulatory performance, Industrial Engineering Chemistry Research 36 (1997) 5339-5347.

[11] R. Monroy-Loperena, I. Cervantes, A. Morales, J. Alvarez-Ramirez, Robustness and parameterization of the proportional plus double-integral compensator, Industrial Engineering Chemistry Research 38 (1997) 2013-2021.

[12] K.M.Passino, Biomimicry of bacterial foraging for distributed optimization and control, IEEE Control System Magazine 22 (3) (2002) 52-67.

[13] Janardan Nanda, S. Mishra, Lalit Chandra Saikia, Maiden Application of Bacterial Foraging-Based optimization technique in multi-area Automatic Generation Control, IEEE Transactions on Power Systems 24(2) (2009) 602-609.

[14] M.M.Adibi, J.N. Borkoski, R.J.Kafka, T.L. Volkmann, Frequency Response of Prime Movers during Restoration, IEEE Transactions on Power Systems, 14 (2) (1999) 751-756.

[15] M.M.Adibi, R.J.Kafka, Power System Restoration Issues, IEEE Computer Applications in Power 4 (2) (1991) 19-24.

[16] J. Hu, Z. Z. Guo, Y. C. Liu, Q. Y. Guo, Power System Restoration and Analysis Of Restoration Sequence of Generating Sets, Power System Technology 28 (18) (2004) 1-4.

[17] Shashi Kant Pandey, Soumya R. Mohanty, Nand Kishor, A literature survey on load–frequency control for conventional and distribution generation power systems, Renewable and Sustainable Energy Reviews 25 (2013) 318–334.

[18] Dimitris Ipsakis, Spyros Voutetakis, Panos Seferlisa, Fotis Stergiopoulos and Costas Elmasides, "Power management strategies for a stand-alone power system using renewable energy sources and hydrogen storage", International Journal of Hydrogen Energy Vol.34, pp 7081-7095, 2009.

[19] Ke´louwani S, Agbossou K, Chahine R, "Model for energy conversion in renewable energy system with hydrogen storage", Journal of Power Sources, 140 (2005) 392–399.

[20] L. Musirin, .N.Dianah, M.Radzi, M. Murtadha Othman, M.Khayat Idris, T. Khawa Abdul Rahman, Voltage Profile Improvement Using Unified Power Flow Controller via Artificial Immune System, WSEAS Transactions on Power System 3(4) (2008) 49-58.

[21] Muwaffaq I. Alomoush, Derivation of UPFC dc load flow model with examples of its use in restructured power systems**,** IEEE Transactions on Power Systems 18 (2003) 1173-1180.

[22] A.Kazemi, M.R. Shadmesgaran, Extended Supplementary Controller of UPFC to Improve Damping Inter-Area Oscillations Considering Inertia Coefficient, International Journal on Energy 2(1) (2008) 432-440.

[23] E. Uzunovic, C.A.Canizares, J.Reeve, Fundamental Frequency Model of Unified Power Flow Controller, North American Power Symposium, NAPS, Cleveland, Ohio, October 1998, pp.23-28.